

Qubitization of Arbitrary Basis Quantum Chemistry by Low Rank Factorization

Dominic W. Berry,^{1,*} Craig Gidney,² Mario Motta,³ Jarrod R. McClean,² and Ryan Babbush^{2,†}

¹*Department of Physics and Astronomy, Macquarie University, Sydney, NSW 2113, Australia*

²*Google Inc., Venice, CA 90291, United States*

³*Division of Chemistry, California Institute of Technology, Pasadena, CA 91125, United States*

(Dated: February 7, 2019)

Recent work has dramatically reduced the gate complexity required to quantum simulate chemistry by using linear combinations of unitaries based methods to exploit structure in the plane wave basis Coulomb operator. Here, we show that one can achieve similar scaling even for arbitrary basis sets (which can be hundreds of times more compact than plane waves) by combining qubitized quantum walks with a low rank factorization of the Coulomb operator. We provide circuits for several variants of our algorithm (which all improve over the best scaling of prior methods) including one with $\tilde{O}(N^{3/2}\lambda)$ T complexity, where N is number of orbitals and λ is the 1-norm of the chemistry Hamiltonian. We deploy our algorithms for simulating the FeMoco molecule (relevant to Nitrogen fixation) and obtain circuits requiring less surface code spacetime volume than prior quantum algorithms for this system, despite us using a larger and more accurate active space.

I. INTRODUCTION

Quantum computers were originally proposed as special purpose tools for efficiently modeling physical quantum mechanical systems [1]. Ever since then quantum simulation has been central to the study of quantum computing [2] while also regarded as one of its most promising applications. In recent years, progress in quantum hardware has led to great optimism for the field. However, a large gap remains between expectations for the technology and the expected value of the relatively few known applications that appear viable on even a small fault-tolerant quantum computer [3]. This disparity has underscored the importance of estimating and reducing the resources required to implement quantum algorithms within a fault-tolerant cost model.

The most widely studied and anticipated application of quantum simulation is chemistry [4]. Most work on this topic has focused on providing solutions to the electronic structure problem by using phase estimation to sample molecular eigenstates and estimate eigenvalues [5, 6]. Even at small problem sizes of around a hundred qubits, efficient and accurate solutions to this problem could prove transformative for various fields of study and the development of technologies such as better batteries, pharmaceuticals and industrial catalysts.

In order to represent molecular systems on a quantum computer one usually discretizes the many-body wavefunction using a basis of single-particle functions referred to as orbitals. The vast majority of quantum chemistry calculations use either plane wave orbitals, or more elaborate orbitals that are commonly composed of linear combinations of Gaussians. The accuracy of these representations is fundamentally limited by resolution of the electron-electron cusp, which occurs at all points in space [7]. As a result, one can show that discretization error is refined asymptotically at a rate of $1/N$, regardless of whether N is the number of plane wave orbitals [8, 9] or Gaussian orbitals [10, 11]; however, in practice there are very significant differences between these representations.

Plane waves are often chosen in calculations of periodic materials and lead to highly structured Hamiltonians. The work of [12] showed that exploiting this structure leads to asymptotic advantages for quantum algorithms. Today, the two best-scaling quantum algorithms for chemistry in second quantization use plane waves; one has $\mathcal{O}(N^3)$ gate complexity (with small constant factors) [13] and one has $\mathcal{O}(N^2 \log N)$ gate complexity (with large constant factors and more spatial complexity) [14]. But a major limitation to using plane waves in second quantization is that one needs a very large number of spin-orbitals to represent many molecular systems to chemical accuracy. The work of [15] suggests resolving this problem by simulating the plane wave Hamiltonian in first quantization to achieve $\tilde{O}(N^{1/3}\eta^{8/3})$ gate complexity, where η is the number of electrons. With such low scaling in N , one might be able to use an extremely large plane wave basis. Unfortunately, the practicality of that algorithm is unclear because it relies on interaction picture simulation techniques which have never been compiled to explicit circuits [14].

The more obvious remedy to the low resolution of plane waves is to use a more compact basis. Indeed, the majority of proposals for the quantum simulation of chemistry focus on using very compact molecular orbitals. However, using molecular orbitals leads to complex Hamiltonians with coefficients defined in terms of integrals and $\mathcal{O}(N^4)$

* Corresponding author: dominic.berry@mq.edu.au

† Corresponding author: babbush@google.com

distinct terms. As a consequence, the first quantum algorithms in this representation had gate complexity $\mathcal{O}(N^{11})$ [16, 17]. Since then, a large community of researchers has worked to significantly reduce the cost of simulation in this representation through tighter bounds [17–19], better mappings between fermions and qubits [20–24], improved state preparation techniques [25–28], application of new time-evolution strategies [29–31], considerations of fault-tolerant overheads [32–34] and other representational and algorithmic insights [35–40].

The lowest rigorous complexity of prior work on second quantized arbitrary basis chemistry simulation is either the $\tilde{\mathcal{O}}(N^5)$ scaling of [30], or the $\tilde{\mathcal{O}}(\lambda^2)$ scaling of [31], where λ is the 1-norm of the Hamiltonian. However, the [30] algorithm suffers from large constant factors in the scaling, and the approach of [31] scales quadratically worse than post-Trotter methods with respect to the evolution time. In practice, we expect the most competitive prior method would be Trotterization based on [40]; however, the Trotter step size for that approach has not been studied (we expect the approach would scale between $\mathcal{O}(N^4)$ and $\mathcal{O}(N^5)$). These results are challenging to compare directly because the scaling of λ with respect to N depends on whether N is growing towards the thermodynamic (large system) or continuum (large basis) limit. Here we provide an algorithm with $\tilde{\mathcal{O}}(N^{3/2}\lambda)$ T complexity, which appears better than all prior work so long as $\lambda = \Omega(N^{3/2})$, and that is usually the case.

The only prior papers to compile a quantum chemistry algorithm to the level of Clifford + T gates and estimate the resources required within an error-correcting code are [13, 33]. These papers focus on minimizing T complexity or Toffoli complexity because these gates cannot be transversely implemented within practical codes [34, 41]. To implement these gates one must distill magic states or Toffoli states, which takes orders of magnitude more spacetime volume (qubitseconds) than executing Clifford gates and also consumes a very large number of physical qubits [42, 43].

The work of [33] focused on the simulation of an active space of the FeMo cofactor of the Nitrogenase enzyme, aka “FeMoco” (stoichiometry $\text{Fe}_7\text{MoS}_9\text{C}$). FeMoco is the active site for the catalytic conversion of Nitrogen gas into ammonia (fertilizer) in biological processes [44]. This reaction is of great importance; while the mechanism is not understood due to complex electronic structure, biological Nitrogen fixation is significantly more efficient than the industrial alternative. The paper by Reiher *et al.* [33] focused on a 108 qubit active space, and determined that roughly 10^{14} T gates would be required. If implemented in the surface code using gates with 10^{-3} error rates, the most efficient protocols for magic state distillation in this context require roughly 15 qubitseconds [34, 41] of space time volume. At those rates, just distilling the magic states needed for [33] would require roughly five million qubitdecades (e.g., five million qubits running for a decade or a billion qubits running for two weeks), which is not practical.

The work of [13] showed that one could perform similar sized chemistry simulations with roughly 10^8 T gates, but in a plane wave rather than Gaussian basis. By application of techniques from [41] such calculations could be implemented in the surface code at 10^{-3} physical error rates with fewer than a million physical qubits in just hours. But unfortunately, one would probably require at least hundreds of thousands of plane waves to treat FeMoco, so this algorithm is not appropriate. In this paper, we develop an approach that has T counts somewhere in between those discussed in [13] and [33] and is compatible with compact molecular orbitals appropriate for a system like FeMoco.

Our approach is to perform phase estimation directly on a quantum walk [45] generated using qubitization oracles [29], designed to simulate Hamiltonians in the linear combinations of unitaries query model [46]. Our analysis of the phase estimation algorithm is nearly identical to that in [13], which realizes a proposal suggested in [26, 27] based on qubitization [29]. We make heavy use of the unary iteration technique introduced in [13] (see also a similar idea in [47]) as well as the QROM based state preparation and coherent alias sampling technique that was originally developed in [13] and then improved to lower T gate complexity in [48]. Finally, a key aspect of our algorithm is to leverage the low rank nature of the Coulomb operator, using a representation recently discussed in [40].

In the case where we limit the number of ancilla qubits used, mostly using the system qubits as “dirty” ancilla, our algorithm can obtain chemical accuracy for FeMoco with about 2×10^{13} Toffoli gates, using either the active spaces of either Reiher [33] or Li [49]. If we allow a large number of ancilla the number of Toffoli gates is about 1.5×10^{12} for the Reiher orbitals, or 10^{12} for the Li orbitals. Throughout we focus on complexities in terms of Toffoli counts, because the non-Clifford gates we use are exclusively Toffolis. The cost in terms of T gates will be 4 times as large but since we are bottlenecked by Toffolis we can directly distill Toffoli states, which is possible with roughly the same cost of distilling two magic states for T gates [41]. Although we improve upon the distillation space time volume required by [33], at 10^{-3} error rates we still require a hundred thousand qubitdecades of state distillation, which is also impractical. Thus, significant portions of this paper discuss how these costs might be improved.

The paper is organized as follows. In **Section II** we explain how it is possible to truncate the Coulomb operator to low rank. Then in **Section III** we describe the Hamiltonian as a linear combination of unitaries, and how to perform the state preparation and controlled unitary operations. We give detailed calculations of the complexities obtained with the different approaches in **Section IV**, and conclude in **Section V**. In **Appendix A**, **Appendix B** and **Appendix C** we discuss technical details relating to how the qubitization state preparation oracle is implemented. In **Appendix D** we discuss numerics on the low rank factorization of the FeMoco active space. Finally, in **Appendix E** we discuss techniques that can be used to further lower the cost of qubitization based quantum chemistry simulations by leveraging unstructured sparsity that may exist in the Coulomb operator.

II. LOW RANK TENSOR FACTORIZATION OF THE COULOMB OPERATOR

In this section we *review* representations of the Coulomb operator based on low rank tensor decompositions that are central to our approach. These ideas have existed in some form in the classical electronic structure literature for decades [50–55], and were recently discussed in the context of Trotter based electronic structure simulations in [40].

We first define the electronic structure Hamiltonian in an arbitrary second quantized basis as

$$H = \sum_{\sigma \in \{\uparrow, \downarrow\}} \sum_{p, q=1}^{N/2} h_{pq} a_{p, \sigma}^\dagger a_{q, \sigma} + \frac{1}{2} \sum_{\alpha, \beta \in \{\uparrow, \downarrow\}} \sum_{p, q, r, s=1}^{N/2} h_{pqrs} a_{p, \alpha}^\dagger a_{q, \beta}^\dagger a_{r, \beta} a_{s, \alpha} \quad (1)$$

$$= \sum_{\sigma \in \{\uparrow, \downarrow\}} \sum_{p, q=1}^{N/2} T_{pq} a_{p, \sigma}^\dagger a_{q, \sigma} + \sum_{\alpha, \beta \in \{\uparrow, \downarrow\}} \sum_{p, q, r, s=1}^{N/2} V_{pqrs} a_{p, \alpha}^\dagger a_{q, \alpha} a_{r, \beta}^\dagger a_{s, \beta} \quad (2)$$

where a_p^\dagger and a_p are fermionic creation and annihilation operators for spin-orbital $\phi_p(r)$. The scalar coefficients h_{pq} and h_{pqrs} are the one- and two-electron integrals over the basis functions,

$$h_{pq} = \int dr_1 \phi_p^*(r_1) \left(-\frac{\nabla^2}{2} + U(r_1) \right) \phi_q(r_1) \quad h_{pqrs} = \int dr_1 dr_2 \phi_p^*(r_1) \phi_q^*(r_2) V(r_1, r_2) \phi_r(r_2) \phi_s(r_1), \quad (3)$$

where $U(r_1)$ and $V(r_1, r_2)$ are the nuclear and electron-electron potentials, respectively. In Eq. (2) we have implicitly defined T_{pq} and V_{pqrs} with respect to the usual integrals by rearranging the Coulomb operator in so-called “chemist notation” with $a^\dagger a a^\dagger a$ instead of $a^\dagger a^\dagger a a$, and absorbing the factor of 1/2 into the coefficients. Reordering operators according to the fermionic anticommutation relations $\{a_p^\dagger, a_q\} = \delta_{pq}$ also slightly changes the one-body coefficients.

Assuming real basis functions (such as molecular orbitals), T_{pq} and V_{pqrs} are real and have the symmetries¹ [56],

$$T_{pq} = T_{qp}, \quad V_{pqrs} = V_{srqp} = V_{pqsr} = V_{qprs} = V_{qpsr} = V_{rsqp} = V_{rspq} = V_{srpq}, \quad (4)$$

which are important for properties of the tensor decompositions we will discuss. The rank-4 tensor V has $N/2$ elements along each axis and we can reshape V (e.g. using “numpy.reshape”) into an $N^2/4 \times N^2/4$ matrix W which has composite indices pq (representing the first electron) and rs (representing the second electron). The W matrix is symmetric and positive semidefinite. We will diagonalize it as

$$W g^{(\ell)} = \omega_\ell g^{(\ell)}, \quad W = \sum_{\ell=1}^L \omega_\ell g^{(\ell)} \left(g^{(\ell)} \right)^T, \quad (5)$$

where $g^{(\ell)}$ is the ℓ^{th} eigenvector of W having size $N^2/4$ and $\omega_\ell \geq 0$ is its associated eigenvalue. Since we are taking V and hence W to be real, $g^{(\ell)}$ will also be real. The rank of W is denoted L .

If W were of full rank then it would be the case that $L = N^2/4$; however, the integrals that one encounters in molecular electronic structure applications contain considerable structure. As a consequence of this structure, it turns out that W is not full rank, and instead $L \in \mathcal{O}(N)$. The physical basis for this result is the pairwise nature of the Hamiltonian interactions, arising from the Coulomb kernel in a real-space representation. This property is regularly exploited in classical approaches to electronic structure in techniques such as “density fitting” [51, 52] which is commonly performed using a Cholesky decomposition [53–55] (which is similar to the diagonalization in Eq. (5) but is numerically more efficient and permits different left and right eigenvectors).

We use the notation $g_{pq}^{(\ell)}$ to denote the entry of $g^{(\ell)}$ indexed by the composite index pq (the same composite index we used to flatten V into W). The eigenvectors $g^{(\ell)}$ inherit certain symmetry properties of V , with the result that $g_{pq}^{(\ell)}$ is symmetric between p and q . We can express the two-electron operator in terms of $g_{pq}^{(\ell)}$ as

$$\sum_{\alpha, \beta \in \{\uparrow, \downarrow\}} \sum_{p, q, r, s=1}^{N/2} V_{pqrs} a_{p, \alpha}^\dagger a_{q, \alpha} a_{r, \beta}^\dagger a_{s, \beta} = \sum_{\ell=1}^L \omega_\ell \left(\sum_{\sigma \in \{\uparrow, \downarrow\}} \sum_{p, q=1}^{N/2} g_{pq}^{(\ell)} a_{p, \sigma}^\dagger a_{q, \sigma} \right)^2. \quad (6)$$

While common in electronic structure, this representation was first proposed in a quantum computing context in [19]; however, that work did not appear to appreciate the low rank aspect, which was first exploited for advantage in

¹ If one were to perform qubitization on the Hamiltonian of Eq. (2) (as opposed to the more elaborate strategy we present here), the eight-fold symmetry in the integrals would obviously help reduce the cost of the state preparation oracle discussed in later sections.

quantum computing in [40]. Whereas there are $\mathcal{O}(N^4)$ seemingly distinct coefficients on the left side of this equation, there are $\mathcal{O}(N^2L) = \mathcal{O}(N^3)$ distinct coefficients on the right side of the equation. Due to symmetry, the number of independent coefficients for each ℓ is $N^2/8 + N/4$, giving a total number of $L(N^2/8 + N/4)$.

The work of [40] also discussed further factorizations of the Hamiltonian based on the results of [57]. There, they showed that one can also diagonalize and truncate the matrix with elements $g_{pq}^{(\ell)}$ which turns out to have only $\mathcal{O}(\log N)$ significant eigenvalues in certain asymptotic limits. Furthermore, one can rotate into the basis where the operator is diagonal using $\mathcal{O}(N \log N)$ operations. One might think this would be useful for linear combinations of unitaries based quantum simulation, and with sufficient cleverness, that might be the case. However, we do not focus on that second factorization in this work because it adds many intricacies, is less well understood than the first factorization, and might not offer an asymptotic advantage in T complexity for technical reasons related to the improved scaling that comes from using the improved QROM discussed later in this work.

III. LCU BASED SIMULATION

A number of techniques for simulating Hamiltonian evolution are based upon the linear combination of unitaries approach [46, 58]. This approach enables one to achieve a sum of unitaries that yield another unitary operation. Say the operation to perform is given in the form $U = \sum_j w_j U_j$, where w_j are real and positive. First a control register is prepared in the state $\sum_j \sqrt{w_j/\lambda} |j\rangle$, where $\lambda = \sum_j w_j$ is needed for normalization. We call this preparation operation ‘‘PREPARE’’. Then a controlled U_j operation is performed on the target system, an operation we will call ‘‘SELECT’’. The inverse PREPARE operation is performed, then if the control system is measured in the state $|0\rangle$, then the operation U will have been applied to the target system. This operation only has probability $1/\lambda^2$ of success, so to achieve U with unit success probability one can use $\sim \lambda$ steps of oblivious amplitude amplification.

This formalism was generalised by the block encoding, or ‘‘qubitization’’, formalism of [29], where one can take the Hamiltonian to be a linear combination of unitaries, and use quantum signal processing [59] to obtain Hamiltonian evolution. For quantum chemistry, we are typically interested in the eigenvalues of the Hamiltonian. In that case, instead of performing the Hamiltonian evolution, one can instead consider performing phase estimation on a single step from the qubitization formalism of [29]. This step corresponds to expressing the Hamiltonian as a linear combination of unitaries using two PREPARE operations and one SELECT operation, as well as a reflection as one would do for oblivious amplitude amplification. The eigenvalues of this step will then be $e^{\pm i \arccos(E_k/\lambda)}$, where E_k are the eigenvalues of the Hamiltonian. The complexity is fundamentally dependent on the quantity $\lambda = \sum_j w_j$. The overall complexity will be proportional to λ multiplied by the complexity of the SELECT and PREPARE operations.

A. The Hamiltonian as a linear combination of unitaries

We can map $a_p^\dagger a_q$ and n_p to qubits using the Jordan-Wigner transformation as

$$a_{p,\sigma}^\dagger a_{q,\sigma} \mapsto \left(X_{p,\sigma} \vec{Z} X_{q,\sigma} + Y_{p,\sigma} \vec{Z} Y_{q,\sigma} \right), \quad a_{p,\sigma}^\dagger a_{p,\sigma} \mapsto \frac{1}{2} (\mathbb{1} - Z_{p,\sigma}), \quad (7)$$

where X , Y and Z are the Pauli operators, the subscripts indicate the qubits these operators act on, and $A_p \vec{Z} A_q$ is shorthand for $A_p Z_{p+1} \cdots Z_{q-1} A_q$. Thus, our Hamiltonian can be represented as the linear combination of unitaries:

$$\begin{aligned} H \mapsto & \frac{1}{2} \sum_{p \neq q, \sigma} T_{pq} \left(X_{p,\sigma} \vec{Z} X_{q,\sigma} + Y_{p,\sigma} \vec{Z} Y_{q,\sigma} \right) + \frac{1}{2} \sum_{p,\sigma} T_{pp} (\mathbb{1} - Z_{p,\sigma}) \\ & + \frac{1}{4} \sum_{\ell} \omega_{\ell} \left(\sum_{p \neq q, \sigma} g_{pq}^{(\ell)} \left(X_{p,\sigma} \vec{Z} X_{q,\sigma} + Y_{p,\sigma} \vec{Z} Y_{q,\sigma} \right) + \sum_{p,\sigma} g_{pp}^{(\ell)} (\mathbb{1} - Z_{p,\sigma}) \right)^2. \end{aligned} \quad (8)$$

The terms in the first line in this expression correspond to the one-body operator T , and the terms in the second line corresponds to the factorized two-body operator. Here the ranges of the summations are the same as for H .

Given the Hamiltonian expressed as a linear combination of unitaries, we can now give the expression for λ . In the following we will use λ_T to refer to the sum of weights for the one-body term as in Eq. (2), and use λ_W to refer to the sum of weights for Coulomb operator in its factorized form, as on the right-hand side of Eq. (6). We have

$\lambda = \lambda_T + \lambda_W$, with

$$\lambda_T = 2 \sum_{p,q=1}^{N/2} |T_{pq}|, \quad \lambda_W = 4 \sum_{\ell=1}^L \omega_\ell \left(\sum_{p,q=1}^{N/2} |g_{pq}^{(\ell)}| \right)^2. \quad (9)$$

Here the factors of 2 and 4 in front of the sums are due to summation over the up and down spins. By simulating the factorized Hamiltonian we are slightly increasing λ over what it would be if we used the Hamiltonian in its original form from Eq. (2). Denoting by λ_V the sum of weights for the potential term in the form Eq. (2), one has

$$\lambda_V = 4 \sum_{p,q,r,s=1}^{N/2} |V_{pqrs}| = 4 \sum_{p,q,r,s=1}^{N/2} \left| \sum_{\ell=1}^L \omega_\ell g_{pq}^{(\ell)} g_{rs}^{(\ell)} \right| \leq 4 \sum_{\ell=1}^L \omega_\ell \sum_{p,q,r,s=1}^{N/2} |g_{pq}^{(\ell)}| |g_{rs}^{(\ell)}| = \lambda_W. \quad (10)$$

However, we do not expect any difference between the asymptotic scaling of λ_V and λ_W with respect to N .

Because these quantities directly scale the complexity of our approach, techniques for reducing the effective value of λ are potentially important. One example of such a technique is to modify the Hamiltonian by adding to it a linear combination of n -representability [60] equality constraints that have provably zero expectation value. This strategy was introduced and shown to be effective in Section V of [61]. Other techniques that might be useful for this include mean-field background subtraction [62] and the use of soft pseudopotentials [63]. However, one should make sure that these methods are applied in a way that does not increase the rank of the Coulomb operator, which would be counterproductive for the overall complexity. Note finally that interaction picture techniques [14] do not appear to be helpful here because while $\lambda_V \gg \lambda_T$, the V operator cannot be fast-forwarded.

In order to perform phase estimation via the qubitization/LCU approach, we need to be able to perform the state preparation PREPARE and controlled unitaries SELECT. The techniques to achieve these operations are described in the following subsections.

B. State preparation

The state we would need to prepare is

$$|\psi\rangle = |0\rangle |+\rangle |0\rangle \sum_{p,q,\sigma} \sqrt{\frac{|T_{pq}|}{\lambda}} |\theta_{pq}^{(0)}\rangle |0\rangle |p,q,\sigma\rangle |0\rangle + \sum_{\ell} \sqrt{\frac{\omega_\ell}{\lambda}} |\ell\rangle |+\rangle |+\rangle \sum_{p,q,r,s,\alpha,\beta} \sqrt{|g_{pq}^{(\ell)} g_{rs}^{(\ell)}|} |\theta_{pq}^{(\ell)}\rangle |\theta_{rs}^{(\ell)}\rangle |p,q,\alpha\rangle |r,s,\beta\rangle, \quad (11)$$

where λ is as defined in Eq. (9), $|+\rangle = (|0\rangle + |1\rangle)/\sqrt{2}$, α and β are spin labels, and the $\theta_{pq}^{(\ell)}$ are used to obtain the correct signs on the terms. They are given by

$$\theta_{pq}^{(0)} = \begin{cases} 0, & T_{pq} > 0, \\ 1, & T_{pq} < 0, \end{cases} \quad \theta_{pq}^{(\ell)} = \begin{cases} 0, & g_{pq}^{(\ell)} > 0, \\ 1, & g_{pq}^{(\ell)} < 0. \end{cases} \quad (12)$$

The first register gives ℓ , with $|0\rangle$ reserved for the first term. The first term gives the first two terms in Eq. (8), with the first term in Eq. (8) obtained for $p \neq q$ and the second term obtained for $p = q$. The $|+\rangle$ state on the second qubit selects between $\mathbb{1}$ and $Z_{p,\sigma}$ for $p = q$. We use $p < q$ and $p > q$ to select between $X_{p,\sigma} \vec{Z} X_{q,\sigma}$ and $Y_{p,\sigma} \vec{Z} Y_{q,\sigma}$ for $p \neq q$, in a similar way as in [13]. The second term gives the third term in Eq. (8), with the sums over p, q and r, s yielding the square. The two $|+\rangle$ states in registers 2 and 3 select between $\mathbb{1}$ and $Z_{p,\sigma}$ for $p = q$ and between $\mathbb{1}$ and $Z_{r,\sigma}$ for $r = s$.

There are $(L+1)(N^2/8 + N/4) = \mathcal{O}(N^3)$ unique coefficients, which indicates the state preparation can be performed with similar complexity. Using the QROM and subsampling techniques from [13], the T complexity can be expected to be $\mathcal{O}(N^3 + \log(1/\epsilon))$, where ϵ is the required precision. By using a more sophisticated preparation scheme it will be possible to reduce the number of T gates, as will be described below.

To perform the state preparation, we start with all registers in the $|0\rangle$ state, then perform the following steps.

1. Prepare a superposition over the first register, to produce the state

$$\left(|0\rangle \sqrt{\sum_{p,q} \frac{2|T_{pq}|}{\lambda}} + 2 \sum_{\ell} \sqrt{\frac{\omega_\ell}{\lambda}} |\ell\rangle \sum_{p,q} |g_{pq}^{(\ell)}| \right) |0\rangle |0\rangle |0\rangle |0\rangle |0\rangle |0\rangle. \quad (13)$$

2. Perform a Hadamard on the second register, and a Hadamard on the third register controlled on the state of the first register being $|\ell\rangle$ for $\ell > 0$, giving

$$\left(|0\rangle |+\rangle |0\rangle \sqrt{\sum_{p,q} \frac{2|T_{pq}|}{\lambda}} + 2 \sum_{\ell} \sqrt{\frac{\omega_{\ell}}{\lambda}} |\ell\rangle |+\rangle |+\rangle \sum_{p,q} |g_{pq}^{(\ell)}| |0\rangle |0\rangle |0\rangle |0\rangle \right). \quad (14)$$

3. Prepare a superposition over register six controlled on the first register. For the first register in the state $|0\rangle$, we prepare weights $\sqrt{|T_{pq}|}$, and for $|\ell\rangle$ with $\ell > 0$ we prepare weights proportional to $\sqrt{|g_{pq}^{(\ell)}|}$. The state is then

$$|0\rangle |+\rangle |0\rangle \sum_{p,q,\sigma} \sqrt{\frac{|T_{pq}|}{\lambda}} |0\rangle |0\rangle |p, q, \sigma\rangle |0\rangle + \sqrt{2} \sum_{\ell} \sqrt{\frac{\omega_{\ell}}{\lambda}} |\ell\rangle |+\rangle |+\rangle \sum_{p,q,\alpha} \sqrt{|g_{pq}^{(\ell)}|} \sqrt{\sum_{r,s} |g_{rs}^{(\ell)}|} |0\rangle |0\rangle |p, q, \alpha\rangle |0\rangle. \quad (15)$$

4. Perform another state preparation on register seven, controlled on register one. For register one in the state $|\ell\rangle$ with $\ell > 0$ we prepare weights proportional to $\sqrt{|g_{rs}^{(\ell)}|}$, giving

$$|0\rangle |+\rangle |0\rangle \sum_{p,q,\sigma} \sqrt{\frac{|T_{pq}|}{\lambda}} |0\rangle |0\rangle |p, q, \sigma\rangle |0\rangle + \sum_{\ell} \sqrt{\frac{\omega_{\ell}}{\lambda}} |\ell\rangle |+\rangle |+\rangle \sum_{p,q,r,s,\alpha,\beta} \sqrt{|g_{pq}^{(\ell)} g_{rs}^{(\ell)}|} |0\rangle |0\rangle |p, q, \alpha\rangle |r, s, \beta\rangle. \quad (16)$$

5. Use QROM to output $|\theta_{pq}^{(\ell)}\rangle$ in register four and $|\theta_{rs}^{(\ell)}\rangle$ in register five.

We will allow total error ϵ . Because there are a number of steps, each step will have an allowable error some fraction of ϵ . Here we aim to estimate the leading-order term in the complexity, and the allowable error will only appear in logarithms, so we will simply give $\log(1/\epsilon)$, rather than subdividing the allowable error between the different steps. Throughout we will use \log to indicate logarithms to base 2.

For the state preparation in step 1, the approach in [13] gives complexity in terms of Toffolis $L + \mathcal{O}(\log(1/\epsilon))$. Throughout we quantify the complexity in terms of Toffolis, because it is possible to directly distill magic states for Toffolis, rather than synthesizing them from T gates. The complexity in terms of T gates is multiplied by a factor of 4. The complexity in step will be negligible compared to the complexity of later steps. The second step is just controlled operations on two qubits, and has negligible complexity compared to the other steps.

Steps 3 and 4 are the key steps that have the greatest complexity. A simple method is to use the unary iteration procedure as described in [13] (Section IIIA) combined with the state preparation procedure in [13] (Section IIID). The unary iteration procedure allows us to progressively perform an operation controlled on a register being $|0\rangle$, then $|1\rangle$, and so forth, with the overall complexity of the control in terms of the number of Toffoli gates being L (since there are here $L + 1$ possible values). That unary iteration procedure is performed on the first register, and for each value of the this register, state preparation is performed on the sixth register (for step 3) or the seventh register (for step 4). That approach gives complexity $N^2/4 + \mathcal{O}(\log(1/\epsilon))$ for each ℓ in both steps 3 and 4. In each case the complexity is $N/2 + \mathcal{O}(\log(1/\epsilon))$ for zero on the first register for step 3 only. The total complexity is then $N/2 + LN^2/2 + \mathcal{O}(L \log(1/\epsilon))$. We can significantly reduce the complexity using three techniques.

- A) Take advantage of the symmetry of $g_{pq}^{(\ell)}$ and T_{pq} .
- B) Combine the preparation for all values of ℓ together.
- C) Use the QROM of [48] which allows one to further reduce Toffoli complexity at the cost of extra ancilla.

To take advantage of the symmetry, we can initially prepare a state proportional to

$$\sqrt{2} \sum_{p < q} \sqrt{|g_{pq}^{(\ell)}|} |p, q, \alpha\rangle + \sum_p \sqrt{|g_{pp}^{(\ell)}|} |p, p, \alpha\rangle \quad (17)$$

Then we have this state tensored with a register in a $|+\rangle$ state. For preparation on register six, the $|+\rangle$ state is on register two (step 3), or for preparation on register seven the $|+\rangle$ state is on register three (step 4).

We can then perform a swap between the registers storing p and q controlled by this register, giving state

$$\sum_{p < q} \sqrt{|g_{pq}^{(\ell)}|} |0\rangle |p, q, \alpha\rangle + \sum_{p > q} \sqrt{|g_{pq}^{(\ell)}|} |1\rangle |p, q, \alpha\rangle + \sum_p \sqrt{|g_{pp}^{(\ell)}|} |+\rangle |p, p, \alpha\rangle \quad (18)$$

This gives the correct weighting for each of the terms in the superposition. As always with these state preparations for LCU, the prepared state is permitted to be entangled with junk registers. For $p \neq q$ the additional ancilla may be regarded as a junk register, whereas for $p = q$ this register will be used to distinguish between $\mathbb{1}$ and $Z_{p,\alpha}$ operations. The controlled swap costs $\log N$ Toffolis, which is negligible compared to other steps. As a result of this simplification, there are $(L + 1)(N^2/8 + N/4)$ distinct values required in step 3, and $L(N^2/8 + N/4)$ distinct values in step 4.

The state preparation is performed in the following way.

- (i) Create an equal superposition over j for the register where we are performing the state preparation.
- (ii) Output alternate indices ($|\text{alt}_j\rangle$ in [13]) and probabilities ($|\text{keep}_j\rangle$ in [13]) using a QROM.
- (iii) Perform an inequality test between the probability register and an ancilla in an equal superposition state.
- (iv) Perform a controlled swap between the register where we are performing the state preparation and the alternate index register based on the result of the inequality test.

We also need to create superpositions over the spin registers, but that can be done trivially with Hadamards. If we were to iterate through ℓ and perform state preparation for each value of ℓ , we would be performing the entire procedure for each value of ℓ . The insight here is to note that we can call the QROM for all ℓ , then perform the inequality test and controlled swap. That means we only need to perform the inequality test and controlled swap once, instead of L times.

The costs of the steps are as follows.

- (i) Creating the equal superpositions is not completely trivial, because we are creating equal superpositions for $p \leq q$. It can be performed using an inequality test and amplitude amplification, with an overall cost $\mathcal{O}(\log(N/\epsilon))$ which is negligible compared to the other costs in the algorithm.
- (ii) The cost of outputting $(L + 1)(N^2/8 + N/4)$ or $L(N^2/8 + N/4)$ numbers in QROM, with outputs of size $\log(N^2) + \log(1/\epsilon) + \mathcal{O}(1)$. Here $\log(N^2)$ is the size of the register for the alternate values, and the size of the register for the probability is $\log(1/\epsilon) + \mathcal{O}(1)$.
- (iii) The inequality test has Toffoli cost of $\log(1/\epsilon) + \mathcal{O}(1)$.
- (iv) The controlled swap has cost $\log(N^2) + \mathcal{O}(1)$.

The dominant cost in this procedure is that of the QROM, which has cost of $(2L + 1)(N^2/8 + N/4)$ Toffolis if we use the procedure of [13]. However, the complexity in terms of Toffolis can be reduced by using a more advanced QROM based on that of [48]. This QROM uses a combination of the QROM of [13] and a technique for trading between spatial complexity and gate complexity in a fashion that accomplishes something reminiscent of what authors aspired to demonstrate with the original concept of ‘‘QRAM’’ [64]. Thus, here we will refer to the more advanced QROM of [48] as ‘‘QROAM’’. In the following we will use d for the number of entries that we must look up using the QROM (here we have $d \approx L(N^2/8 + N/4)$), k for an arbitrary power of two, and M for the size of the output in qubits (here we have $M = \log(N^2/\epsilon) + \mathcal{O}(1)$). Then the complexity for computing the QROM is $d/k + 2Mk$ (see Appendix A), and for uncomputing the QROM is $d/k + k$ (see Appendix C). Moreover, it is possible to choose the k for the uncompute to be different from that for the compute step. The number of additional ancillae needed is $(k - 1)M$. It is also possible to use ancillae that are already being used for some other purpose, called ‘‘dirty’’ ancillae. Using these dirty ancillae, the compute cost is almost twice as much, $2d/k - 2M + 4Mk$ (see Appendix B), and the uncompute cost is changed to $2d/k + 4k$. The compute and uncompute are used for the state preparation and inverse state preparation, so the combined cost is what needs to be considered.

We will consider two cases. First is that where we attempt to minimize the cost in terms of Toffolis, but use a large number of ancillae. In that case, for the compute we can take $k \approx \sqrt{d/2M}$, in which case the cost of the compute step is approximately $2\sqrt{2dM}$. For the uncompute, we can take $k \approx \sqrt{d}$, which gives an uncompute cost of approximately $2\sqrt{d}$, for a total cost of the compute and uncompute of $2\sqrt{d}(\sqrt{2M} + 1)$. For our $d \approx LN^2/8$ and $M \approx \log(N^2/\epsilon)$, we get a combined cost of approximately

$$\sqrt{LN^2 \log(N^2/\epsilon)}. \quad (19)$$

We find that this approach needs a number of extra ancillae

$$\frac{1}{4}\sqrt{LN^2 \log(N^2/\epsilon)}. \quad (20)$$

As $L = \mathcal{O}(N)$ the complexity in terms of Toffolis is $\mathcal{O}(N^{3/2}\sqrt{\log(N/\epsilon)})$, and a similar number of ancillae are needed.

Alternatively, if we are attempting to minimize the number of additional ancillae needed, we can use dirty ancillae instead. Fortunately, we happen to have N dirty ancilla lying around because the system register is not acted upon while implementing the state preparation operation. Moreover, there are multiple steps of state preparation that are performed, and there are qubits that will be used in some steps of state preparation that can be used as dirty qubits for the other steps of state preparation. We will find that we can take the number of dirty qubits to be somewhat larger than N , but not a lot larger. Assuming the number of dirty qubits is about N , we can take $k \approx N/M$. Then we would have compute cost $2dM/N - 2M + 4N \approx \frac{1}{4}LN \log(N^2/\epsilon)$. For the uncompute step we can take $k \approx N$, giving cost approximately $LN/4$. In both cases the costs need to be multiplied by 2 to account for steps 3 and 4.

Finally we consider the cost of outputting $|\theta_{pq}^{(\ell)}\rangle$ in register four and $|\theta_{rs}^{(\ell)}\rangle$ in register five. This use of QROM can simply be combined with that in steps 3 and 4. For example, for step 3, when calling the QROM for the state preparation, output the value of $\theta_{pq}^{(\ell)}$, as well as that for the alternate values of p and q . Then, when doing the controlled swap, also swap these registers. There is a net increase in the size of the output of 2 qubits, and one extra Toffoli for the controlled swaps. This cost is negligible compared to the overall cost in steps 3 and 4.

C. Controlled unitaries

For the controlled unitaries (the SELECT circuit) in the case of using only the first diagonalization, we need to implement the terms in the Hamiltonian as in Eq. (8). The general principle is that we do a pair of operations, each of which has $X_p \vec{Z} X_q$ and $Y_p \vec{Z} Y_q$ for $p \neq q$, with the term selected by whether p or q is larger. For $p = q$ we use an ancilla qubit to select between $\mathbb{1}$ and Z_p . The way the state preparation is chosen, this can be performed in the same way for $\ell = 0$ and $\ell > 0$, because the ancillae will only select the identity operation. The operations we need are

$$\begin{aligned} & \text{SELECT}_1 |q_1, q_2, \theta_1, \theta_2, \{p, q, \alpha\}, \{r, s, \beta\}\rangle |\psi\rangle \\ &= (-1)^{\theta_1} |q_1, q_2, \theta_1, \theta_2, \{p, q, \alpha\}, \{r, s, \beta\}\rangle \otimes \begin{cases} X_{p,\alpha} \vec{Z} X_{q,\alpha} |\psi\rangle, & p < q, \\ Y_{p,\alpha} \vec{Z} Y_{q,\alpha} |\psi\rangle, & p > q, \\ |\psi\rangle, & p = q \wedge q_1 = 1, \\ -Z_{p,\alpha} |\psi\rangle, & p = q \wedge q_1 = 0, \end{cases} \end{aligned} \quad (21)$$

$$\begin{aligned} & \text{SELECT}_2 |q_1, q_2, \theta_1, \theta_2, \{p, q, \alpha\}, \{r, s, \beta\}\rangle |\psi\rangle \\ &= (-1)^{\theta_2} |q_1, q_2, \theta_1, \theta_2, \{p, q, \alpha\}, \{r, s, \beta\}\rangle \otimes \begin{cases} X_{r,\beta} \vec{Z} X_{s,\beta} |\psi\rangle, & r < s, \\ Y_{r,\beta} \vec{Z} Y_{s,\beta} |\psi\rangle, & r > s, \\ |\psi\rangle, & r = s \wedge q_2 = 1, \\ -Z_{r,\beta} |\psi\rangle, & r = s \wedge q_2 = 0. \end{cases} \end{aligned} \quad (22)$$

Note that the selected operations we need are similar to those in [13, 65], and we can use a similar approach. The complexity is linear in N , and will therefore be smaller than the complexity of the state preparation. The technique is shown in Figure 1 for SELECT_1 , and SELECT_2 is equivalent. If $p < q$ then the Y operation in $Z \dots ZY$ acts on the same qubit as one of the Z s in the $Z \dots ZX$ operation. As a result, the Y gets multiplied by Z and becomes $ZY = -iX$. Therefore the operation implemented is of the form $-iX_{p,\alpha} \vec{Z} \dots ZX_{q,\alpha}$. If $p > q$ then the X operation in $Z \dots ZX$ acts on the same qubit as one of the Z s in the $Z \dots ZY$ operation. Thus we have X times Z on that qubit giving $XZ = -iY$. Therefore the operation implemented is of the form $-iY_p Z \dots ZY_q$. If $p = q$ then all the Z s cancel leaving only $X_{p,\alpha} Y_{p,\alpha} = iZ_{p,\alpha}$.

Now note that the register q_1 is 0 for $p < q$ and 1 for $p > q$. Before and after the ranged operations, we perform an inequality test between p and q , controlled on q_1 , with the result that an extra ancilla is in the state $|1\rangle$ unless $p = q$ and $q_1 = 0$. That register is used as a control for the ranged operations, so if $p = q$ and $q_1 = 0$ then the identity is performed. We then apply an S gate on this ancilla, with the result that the operations performed are $X_{p,\alpha} Z \dots ZX_{q,\alpha}$ for $p < q$, $Y_{p,\alpha} Z \dots ZY_{q,\alpha}$ for $p > q$, and $-Z_{p,\alpha}$ for $p = q$ and $q_1 = 0$. For $p = q$ and $q_1 = 0$ this ancilla is zero, so the phase on the identity is unchanged. This yields the desired operations with the correct phases, and lastly the controlled Z on the θ register gives the $(-1)^{\theta_1}$ phase factor.

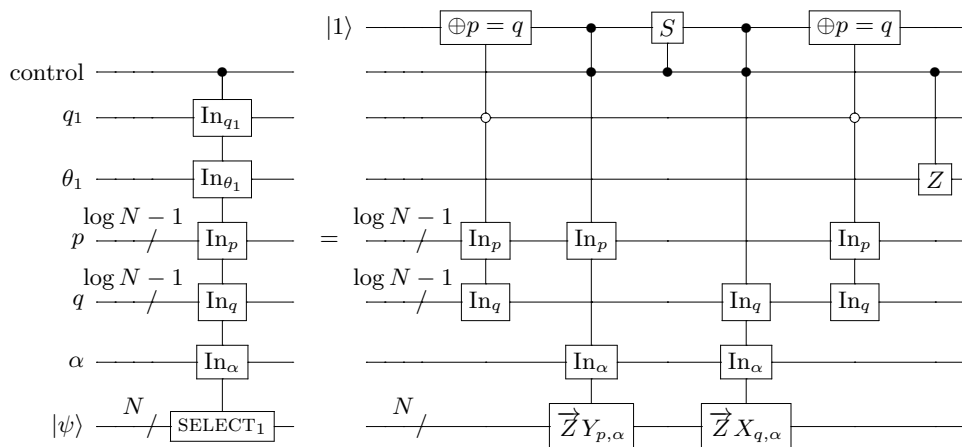


FIG. 1. The circuit needed to perform a controlled SELECT_1 operation. We have omitted the registers this operation does not act upon for simplicity. The unitaries labeled as $\vec{Z}A_j$ apply the operation $Z_0 \cdots Z_{j-1}A_j$ to the target register, depending on the value from the input register, using the technique shown in Figure 9 of [13]. This operation can be achieved using an inequality test, followed by a ranged operation via the technique shown in Figure 8 of [13]. The controlled SELECT_2 operation is completely equivalent except with different control registers.

IV. COMPLEXITY

Let us denote the upper bound on the error required for the eigenvalue estimation by ΔE . Then following [13] we find the complexity of the estimation is the cost of each LCU step times 2^m , where

$$m = \left\lceil \log \left(\frac{\sqrt{2}\pi\lambda}{2\Delta E} \right) \right\rceil. \quad (23)$$

Moreover, the error that is allowable for the implementation of each LCU step is

$$\epsilon = \frac{\sqrt{2}\Delta E}{4\lambda}. \quad (24)$$

A. Reiher *et al.* orbitals

The prominence of the Reiher *et al.* paper [33], which was the first work to rigorously estimate the T complexity of any quantum algorithm for chemistry makes it an important benchmark. However, unfortunately, Li *et al.* [49] later argued that there were substantial problems with the orbitals chosen for Reiher *et al.* paper. For the reasons discussed in the paper by Li *et al.*, we believe that future papers should compare against this work using only the Li integrals. But in order to more easily compare with past work, here we analyze the complexity of simulating both Reiher *et al.* and Li *et al.* FeMoco active spaces. Note that at 152 spin-orbitals the Li active space is also significantly larger than the 108 spin-orbital Reiher active space. For both active spaces, we will focus on obtaining the standard “chemical accuracy”, corresponding to $\Delta E = 0.0016$ a.u. [56].

For the integrals of Reiher *et al.*, $\lambda_T = 1,490$ a.u. and $\lambda_W = 34,552$ a.u., for a total of $\lambda = 36,042$ a.u. That gives $\epsilon \approx 1.7 \times 10^{-8}$. The output size for the QROM is approximately $\log(N^2/\epsilon)$ for $N = 108$, giving about 40. More specifically, the output size for the probabilities in the QROM is given by Eq. (36) in [13]. In that equation, only the first term is significant, giving

$$\mu = \left\lceil \log \left(\frac{2\sqrt{2}\lambda}{\Delta E} \right) \right\rceil. \quad (25)$$

That would give $\mu = 26$ bits, except we have three steps of state preparation, which means the number of qubits for the probabilities needs to be increased by 2 to $\mu = 28$. With $N = 108$ we need two registers of size $\lceil \log(N/2) \rceil = 6$, as well as two single qubit registers for the θ values, for a total of $M = 42$ qubits for steps 3 and 4.

For FeMoco, we have performed computations with MP2 and CISD with various values of L , and found that the error due to the truncation is within chemical precision for $L \geq 200$ (see Appendix D). For step 1 (preparing the

superposition over the ℓ register, only 8 qubits are needed for ℓ , for a total of 36 qubits output. We will use the QROAM for steps 3 and 4, as these steps have the dominant complexity.

1. Dirty ancillae

If we are attempting to minimize the number of qubits used, it is convenient to combine steps 1 and 3. That is, we use a state preparation over ℓ , p , and q simultaneously, and output all values for these three indices. Then there are only two steps of state preparation, and we can reduce the number of qubits for the keep probabilities to $\mu = 27$. That means the state preparation has an output size of $M_1 = 8 + 12 + 2 + 27 = 49$. There will be $M_2 = 41$ qubits used for the output in step 4, because there is one fewer qubit for the keep probability.

If we use dirty qubits, then in the first state preparation we can use the $N = 108$ system registers as well as the $M_2 = 41$ ancilla registers that will be used as output in the next step. We can therefore take $k = 4$, which uses $(k - 1)M_1 = 147$ qubits, and fits within that size. Similarly, for the second state preparation, we are able to use the output registers from the first state preparation as dirty qubits. The cost of the QROAM compute would be $d/2 + 14M$. For the uncompute, we can take $k = 128$, giving cost $2d/k + 4k = d/64 + 512$.

Taking $L = 200$ gives $d_1 = (L + 1)(N^2/8 + N/4) = 298,485$ for the first preparation, and

$$d_1/2 + 14M_1 + d_1/64 + 512 = 155,105. \quad (26)$$

For the second state preparation $d_2 = L(N^2/8 + N/4) = 297,000$, giving

$$d_2/2 + 14M + d_2/64 + 512 = 154,227. \quad (27)$$

The total is 309,332. We find that the number of qubits for the phase estimation is

$$m = \left\lceil \log \left(\frac{\sqrt{2}\pi\lambda}{2\Delta E} \right) \right\rceil = 26, \quad (28)$$

so we obtain an overall complexity (in terms of Toffolis)

$$2^m \times 309,332 \approx 2.1 \times 10^{13}. \quad (29)$$

Next we consider the number of ancilla qubits used. As well as the $49 + 41 = 90$ qubits we have used as output in the two steps of the state preparation, we need the following qubits.

1. Each state preparation needs μ qubits to store a superposition state to perform the inequality comparison.
2. We are preparing a state with a number of qubits

$$\lceil \log L \rceil + 4 + 4\lceil \log(N/2) \rceil = 36. \quad (30)$$

In this expression the first term takes account of ℓ , the +4 takes account of q_1, q_2, α , and β , and the last term takes account of the p, q, r, s registers.

3. The number of qubits needed for the phase estimation $m = 26$.

Adding all these qubit counts together gives 206.

2. Large ancilla count

Alternatively, we can use a large number of ancilla qubits in an attempt to minimize the Toffoli count. In the compute step it is optimal to take $k = 64$, and in the uncompute step it is optimal to take $k = 512$. The combined complexity of compute and uncompute for each step is then

$$d/64 + 128M + d/512 + 512. \quad (31)$$

In this case it is better to use steps 3 and 4 as described above, with a separate state preparation for ℓ in step 1. Since there are three steps of state preparation, we should take $M = 42$. With the d values given above, we obtain a

complexity 11,135 for step 3 and 11,109 for step 4, for a total of 22,244. That gives an overall complexity in terms of Toffolis

$$2^m \times 22,244 \approx 1.5 \times 10^{12}. \quad (32)$$

The number of ancillae used in the QROAM is approximately

$$kM = 2,688. \quad (33)$$

We use that in step 3, and will erase all but M of the registers. Then we need 2,688 qubits again in step 4. We can erase those registers again, and use some of those qubits for the registers for the inequality test with the keep probability registers, so the qubits for those registers do not add to the overall qubit count. We also need 64 qubits for the state preparation in step 1 (with 8 qubits for alt values, and two size $\mu = 28$ registers). We again need 36 qubits for the system registers, and 26 for the phase estimation registers, for a total of 2,856.

B. Li *et al.* orbitals

An alternative active space for FeMoco was advocated for in [49]. This work argued that the active space Hamiltonian from Reiher *et al.* did not properly capture the electronic structure of FeMoco and was classically solvable. Li *et al.* introduced an alternative Hamiltonian the FeMoco active space with $N = 152$ spin-orbitals. There it is found that $\lambda_T = 3,446$ a.u. and $\lambda_W = 20,746$ a.u., for a total of $\lambda = 24,192$ a.u.. The smaller value of λ means that the number of qubits for the probabilities should be $\mu = 27$ regardless of whether we merge steps 1 and 3 or not. Since N is larger than before, we now need one additional qubit for each of the orbital numbers, for a total of $M = 43$ qubits.

1. Dirty ancillae

Merging steps 1 and 3, the output size is $M_1 = 51$ for the first state preparation, then $M_2 = 43$ for the second state preparation. This time taking $k = 4$ would use $(k-1)M_1 = 153$ qubits for the first state preparation and $(k-1)M_2 = 129$ for the second, both of which are small enough to use other qubits as dirty qubits. We again can take $L = 200$ which results in $d_1 = (L+1)(N^2/8 + N/4) = 588,126$ for the first preparation and $d_2 = L(N^2/8 + N/4) = 585,200$ for the second preparation (step 4). Using $k = 128$ for the uncompute again yields a cost for the first preparation of

$$d_1/2 + 14M_1 + d_1/64 + 512 = 304,479. \quad (34)$$

The cost of the second preparation is approximately

$$d_2/2 + 14M_2 + d_2/64 + 512 = 302,858. \quad (35)$$

That gives a total of 607,337. This time we find that $\log(\sqrt{2\pi\lambda}/(2\Delta E))$ is very slightly larger than 25

$$\log\left(\frac{\sqrt{2\pi\lambda}}{2\Delta E}\right) \approx 25.0015. \quad (36)$$

It would be unreasonably inefficient to round up to $m = 26$. Instead we can allow very slightly less error in other parts of the algorithm (which does not affect the complexity significantly because the algorithm depends on that error logarithmically) and take $m = 25$. Then we get a total cost

$$2^m \times 607,337 \approx 2.0 \times 10^{13}. \quad (37)$$

This time the ancillae used are as follows.

1. The two QROMs use $51 + 43 = 94$ qubits.
2. The two size $\mu = 27$ registers for the inequality tests.
3. The number of qubits in the prepared state is $\lceil \log L \rceil + 4 + 4\lceil \log(N/2) \rceil = 40$.
4. The number of qubits for the phase estimation is $m = 25$.

The total number of ancillae is 213.

2. Large ancilla count

If we use a large number of ancilla qubits, we should again take the k sizes as 64 and 512 in the compute and uncompute steps, respectively. We again perform steps 1 and 3 separately in this case. The M will be 43 for both steps 3 and 4. Then using $d/64 + 128M + d/512 + 512$ gives Toffoli costs 16,355 and 16,303 for steps 3 and 4, respectively, for a total of 32,658. That gives an overall complexity in terms of Toffolis

$$2^m \times 32,658 \approx 1.1 \times 10^{12}. \quad (38)$$

The number of ancillae used in step 4 is approximately

$$kM \approx 2,752. \quad (39)$$

The other ancillae used are as follows.

1. The $M = 43$ qubits used in step 3 that are not erased before step 4.
2. The 62 qubits used for the state preparation in step 1.
3. The 40 system registers.
4. The 25 control qubits for state preparation.

The registers for the inequality tests can again be taken to be qubits for the QROAM that have been erased. The total number of qubits is therefore 2,922.

In summary, the Toffoli costs are as given in Table I. In this table we have given approximate formulae including only the leading terms, and taken $k = 4$ for the QROM compute circuits.

V. DISCUSSION

The cost of performing Toffoli gates may be estimated as follows. The efficient CCZ factory from [41] has a rectangular footprint of 12×8 logical qubit patches. The paper specifies a code distance of $d = 31$ which, in the rotated surface code, means each patch covers $2 \cdot 31^2 \approx 2000$ physical qubits. The factory outputs a CCZ states every $5.5d$ cycles which, assuming a surface code cycle time of 1 microsecond, is once every 170 microseconds. Thus the spacetime volume of the factory is $2000 \cdot (12 \times 8)$ physical qubits times 170 microseconds which equals roughly 30 qubitseconds. Every Toffoli we perform requires at least this much spacetime volume. With the same overhead one can use these techniques to produce two magic states.

The Toffoli counts that we report in Table I are on the order of a trillion. Combined with the 30 qubitsecond spacetime volume for distilling a CCZ state, the spacetime volume of the algorithm is trivially at least 350 megaqubitdays. For context, 350 megaqubitdays of spacetime volume means that if we use “only” a million physical qubits then the computation must run for at least 350 days. Conversely, if we want the computation to finish in a day, we need at least 350 million qubits. We want computations to finish in less than a day, and we don’t want to use hundreds of millions of qubits. This implies that, when attempting to move our algorithm into the regime of practical computations, we should focus on optimizations that reduce spacetime volume (such as exploiting symmetries in the Hamiltonian to reduce the size of QROM reads) instead of optimizations that convert spacetime volume (such as performing parallel distillation of states, which reduces time at the cost of space).

| | Toffolis for dirty ancilla algorithm | logical qubits for dirty ancilla algorithm | Toffolis for many ancilla algorithm | logical qubits for many ancilla algorithm |
|-------------------------------------|--|--|--|---|
| leading order scaling | $\sqrt{2}\pi\lambda N^2 L / (8\Delta E)$ | $N + \log(L^2 N^8) + 4\mu + m$ | $2\sqrt{2}\pi\lambda N \sqrt{LM} / \Delta E$ | $N + N\sqrt{LM} / 4$ |
| Reiher integrals [33] ($N = 108$) | 2.1×10^{13} | 206 | 1.5×10^{12} | 2,856 |
| Li integrals [49] ($N = 152$) | 2.0×10^{13} | 213 | 1.1×10^{12} | 2,922 |

TABLE I. The leading order Toffoli and spatial complexities for the algorithms using dirty ancilla or allowing a large ancilla count. The formulae given are approximate, with the counts determined in a more exact way explained in the text. Here N is the number of spin-orbitals, L is the rank of the Coulomb operator, λ is the 1-norm of the Hamiltonian as defined in Eq. (9), ΔE is the target precision for phase estimation, k is a block size used in the QROAM, M is the output size for the QROAM, μ is the number of qubits used for “keep” probabilities, and m is the number of qubits used for the phase estimation.

While our many ancilla algorithm has $\mathcal{O}(N^{3/2})$ spatial complexity and would require a few thousand logical qubits to simulate FeMoco, we note that at 350 megaqubitdays of spacetime volume just for state distillation, our algorithm is certainly bottlenecked by the Toffoli complexity, and not by the logical qubit costs. Thus, despite the increased spatial costs, we regard the many qubit algorithm as more practical than the dirty ancilla algorithm. In fact, the current overhead of state distillation is so high that one might wonder if there are other techniques that could be used to reduce the Toffoli count at the expense of extra ancilla. In our algorithm, the Toffolis are coming from our use of QROM. Unfortunately, a lower bound proven in [48] suggests that no further tradeoffs of this type will be possible that asymptotically reduce the Toffoli count of the QROM we are using.

One approach to reducing the overall cost would be to exploit structure in the Hamiltonian that further reduces the effective number of coefficients that must be read from QROM. In Appendix E we present one such strategy based on leveraging sparsity in the Coulomb operator. In some cases sparsity in the Hamiltonian arises due to locality of interactions (for large systems) [66], but sparsity also arises for reasons having to do with the symmetry point groups of molecules in real space and the symmetry point groups of molecular orbitals in an active space (this would likely be the origin of sparsity in the FeMoco active space, for instance). It might also be possible to exploit these symmetries (which are embedded in the V_{pqrs} or $g_{pq}^{(\ell)}$ tensors) using techniques from group theory.

Another avenue for reducing the total cost would be to reduce the size of the λ parameter. For example, a technique described in Section V of [61] may help reduce the λ parameter by exploiting n -representability conditions. Another approach might be to incorporate mean-field background subtraction [62]. One could also explore options for selecting the active space differently. For instance, by using different orbitals that are more local, or more symmetric, one could potentially induce more sparsity in the Hamiltonian. Or, one could try to select active space orbitals with a goal of reducing λ . In both of these contexts, the use of pseudopotentials might help [63].

For the purpose of simulating arbitrary basis chemistry Hamiltonians, our approach is certainly the best scaling (and perhaps most practical) shown to date. Despite us using a larger and more accurate active space, we have certainly improved over the 10^{14} T gates required by [33]. Using the techniques from [41] (which are currently state-of-the-art), two magic states can be produced using 30 qubitseconds of space time volume. Thus, a lower bound on the spacetime volume of the [33] algorithm would require 17 gigaqubitdays of state distillation, which is fifty times more than our approach. To be fair, we recognize that this comparison ignores storage, routing, and Clifford operations; however, costs are still so high that we do not think it is worthwhile to perform a complete surface code layout.

Of course, it might be the case that the best path forward uses a different algorithm or representation entirely. One intriguing recent algorithm is the randomized compiled Trotter algorithm of [31], which performs time evolution at a cost of $\mathcal{O}(\lambda^2 t^2 / \epsilon)$ where t is evolution time and ϵ is the diamond norm of the randomized compiled algorithm output with respect to the intended density matrix. Since for the purposes of time-evolution, $t \propto 1/\Delta E$, a lower bound on the T count for FeMoco would be $\lambda^2/\Delta E^2$ which is more than 10^{13} , and we have ignored the cost of rotation synthesis as well as constant factors from phase estimation (which would likely increase the T count by at least a factor of 100).

Another interesting possibility is that Trotterization based on the Trotter step of [40] would provide a significant improvement over the Trotter results in [33]. In practice, Trotter errors depend sensitively on the structure of the Trotter step, and this has not yet been analyzed for the approach of [40]. However, this seems like a promising direction. In that context one might also wonder if using higher-order Trotter formulas could further bring down the costs, as observed for simulating simpler models in [47].

Given the disappointingly high overhead that appear to be required for simulating FeMoco in a molecular orbital basis, we might wonder how practical it would be to perform the simulation in the plane wave basis. No approach based on second quantization is sensible here because one would need perhaps $N = 10^6$ plane waves to simulate a FeMoco active space to sufficiently high accuracy. However, the first quantized algorithm of [15] continues to look competitive. While the constant factors still need to be worked out, that approach scales as $\tilde{\mathcal{O}}(N^{1/3}\eta^{8/3}/\Delta E)$ where the number of electrons is η . If $N = 10^6$, $\eta = 54$ (as in the Reiher active space) and $\Delta E = 0.0016$ a.u., the quantity $N^{1/3}\eta^{8/3}/\Delta E$ is roughly 10^9 . Thus, if further symmetries can be exploited in this simulation to further reduce costs (given that there will be other overheads), we expect this might be a viable way forward; however, more work is clearly needed.

ACKNOWLEDGMENTS

DWB is funded by Australian Research Council Discovery Projects DP160102426 and DP190102633. The authors thank Garnet Kin-Lic Chan, Austin Fowler, and Hartmut Neven for helpful discussions.

-
- [1] R. P. Feynman, *International Journal of Theoretical Physics* **21**, 467 (1982).
- [2] S. Lloyd, *Science* **273**, 1073 (1996).
- [3] M. Mohseni, P. Read, H. Neven, S. Boixo, V. Denchev, R. Babbush, A. Fowler, V. Smelyanskiy, and J. Martinis, *Nature* **543**, 171 (2017).
- [4] A. Aspuru-Guzik, A. D. Dutoi, P. J. Love, and M. Head-Gordon, *Science* **309**, 1704 (2005).
- [5] A. Y. Kitaev, [arXiv:9511026](https://arxiv.org/abs/9511026) (1995).
- [6] D. S. Abrams and S. Lloyd, *Physical Review Letters* **79**, 4 (1997).
- [7] T. Kato, *Communications on Pure and Applied Mathematics* **10**, 151 (1957).
- [8] J. Harl and G. Kresse, *Physical Review B* **77**, 45136 (2008).
- [9] J. J. Shepherd, A. Grüneis, G. H. Booth, G. Kresse, and A. Alavi, *Physical Review B* **86**, 35111 (2012).
- [10] T. Helgaker, W. Klopper, H. Koch, and J. Noga, *Journal of Chemical Physics* **106**, 10.1063/1.473863 (1998).
- [11] A. Halkier, T. Helgaker, P. Jørgensen, W. Klopper, H. Koch, J. Olsen, and A. K. Wilson, *Chemical Physics Letters* **286**, 243 (1998).
- [12] R. Babbush, N. Wiebe, J. McClean, J. McClain, H. Neven, and G. K.-L. Chan, *Physical Review X* **8**, 011044 (2018).
- [13] R. Babbush, C. Gidney, D. W. Berry, N. Wiebe, J. McClean, A. Paler, A. Fowler, and H. Neven, *Phys. Rev. X* **8**, 041015 (2018).
- [14] G. H. Low and N. Wiebe, [arXiv:1805.00675](https://arxiv.org/abs/1805.00675) (2018).
- [15] R. Babbush, D. W. Berry, J. R. McClean, and H. Neven, [arXiv:1807.09802](https://arxiv.org/abs/1807.09802) (2018).
- [16] J. D. Whitfield, J. Biamonte, and A. Aspuru-Guzik, *Molecular Physics* **109**, 735 (2011).
- [17] D. Wecker, B. Bauer, B. K. Clark, M. B. Hastings, and M. Troyer, *Physical Review A* **90**, 1 (2014).
- [18] R. Babbush, J. McClean, D. Wecker, A. Aspuru-Guzik, and N. Wiebe, *Physical Review A* **91**, 22311 (2015).
- [19] D. Poulin, M. B. Hastings, D. Wecker, N. Wiebe, A. C. Doherty, and M. Troyer, *Quantum Information & Computation* **15**, 361 (2015).
- [20] J. T. Seeley, M. J. Richard, and P. J. Love, *Journal of Chemical Physics* **137**, 224109 (2012).
- [21] K. Setia and J. D. Whitfield, [arXiv:1712.00446](https://arxiv.org/abs/1712.00446) (2017).
- [22] S. Bravyi, J. M. Gambetta, A. Mezzacapo, and K. Temme, [arXiv:1701.08213](https://arxiv.org/abs/1701.08213) (2017).
- [23] M. Steudtner and S. Wehner, [arXiv:1712.07067](https://arxiv.org/abs/1712.07067) (2017).
- [24] Z. Jiang, J. McClean, R. Babbush, and H. Neven, [arXiv:1812.08190](https://arxiv.org/abs/1812.08190) (2018).
- [25] L. Veis and J. Pittner, *Journal of Chemical Physics* **140**, 1 (2014).
- [26] D. W. Berry, M. Kieferová, A. Scherer, Y. R. Sanders, G. H. Low, N. Wiebe, C. Gidney, and R. Babbush, *npj Quantum Information* **4**, 22 (2018).
- [27] D. Poulin, A. Y. Kitaev, D. Steiger, M. Hastings, and M. Troyer, *Physical Review Letters* **121**, 010501 (2017).
- [28] N. M. Tubman, C. Mejuto-Zaera, J. M. Epstein, D. Hait, D. S. Levine, W. Huggins, Z. Jiang, J. R. McClean, R. Babbush, M. Head-Gordon, and K. B. Whaley, [arXiv:1809.05523](https://arxiv.org/abs/1809.05523) (2018).
- [29] G. H. Low and I. L. Chuang, [arXiv:1610.06546](https://arxiv.org/abs/1610.06546) (2016).
- [30] R. Babbush, D. W. Berry, I. D. Kivlichan, A. Y. Wei, P. J. Love, and A. Aspuru-Guzik, *New Journal of Physics* **18**, 33032 (2016).
- [31] E. Campbell, [arXiv:1811.08017](https://arxiv.org/abs/1811.08017) (2018).
- [32] N. Cody Jones, J. D. Whitfield, P. L. McMahon, M.-H. Yung, R. V. Meter, A. Aspuru-Guzik, and Y. Yamamoto, *New Journal of Physics* **14**, 115023 (2012).
- [33] M. Reiher, N. Wiebe, K. M. Svore, D. Wecker, and M. Troyer, *Proceedings of the National Academy of Sciences* **114**, 7555 (2017).
- [34] D. Litinski, [arXiv:1808.02892](https://arxiv.org/abs/1808.02892) (2018).
- [35] I. Kassal, S. P. Jordan, P. J. Love, M. Mohseni, and A. Aspuru-Guzik, *Proceedings of the National Academy of Sciences* **105**, 18681 (2008).
- [36] B. Toloui and P. J. Love, [arXiv:1312.2579](https://arxiv.org/abs/1312.2579) (2013).
- [37] M. B. Hastings, D. Wecker, B. Bauer, and M. Troyer, *Quantum Information & Computation* **15**, 1 (2015).
- [38] K. Sugisaki, S. Yamamoto, S. Nakazawa, K. Toyota, K. Sato, D. Shiomi, and T. Takui, *The Journal of Physical Chemistry A* **120**, 6459 (2016).
- [39] F. Motzoi, M. P. Kaicher, and F. K. Wilhelm, *Physical Review Letters* **119**, 160503 (2017).
- [40] M. Motta, E. Ye, J. R. McClean, Z. Li, A. J. Minnich, R. Babbush, and G. K.-L. Chan, [arXiv:1808.02625](https://arxiv.org/abs/1808.02625) (2018).
- [41] C. Gidney and A. G. Fowler, [arXiv:1812.01238](https://arxiv.org/abs/1812.01238) (2018).
- [42] A. G. Fowler, M. Mariantoni, J. M. Martinis, and A. N. Cleland, *Physical Review A* **86**, 32324 (2012).
- [43] A. G. Fowler and C. Gidney, [arXiv:1808.06709](https://arxiv.org/abs/1808.06709) (2018).
- [44] H. Beinert, R. Holm, and E. Munck, *Science* **277**, 653 (1997).
- [45] M. Szegedy, in *45th Annual IEEE Symposium on Foundations of Computer Science* (IEEE, 2004) pp. 32–41.

- [46] A. M. Childs and N. Wiebe, *Quantum Information & Computation* **12**, 901 (2012).
- [47] A. M. Childs, D. Maslov, Y. Nam, N. J. Ross, and Y. Su, [arXiv:1711.10980](https://arxiv.org/abs/1711.10980) (2017).
- [48] G. H. Low, V. Kliuchnikov, and L. Schaeffer, [arXiv:1812.00954](https://arxiv.org/abs/1812.00954) (2018).
- [49] Z. Li, J. Li, N. S. Dattani, C. J. Umrigar, and G. K.-L. Chan, *The Journal of Chemical Physics* **150**, 024302 (2019).
- [50] E. G. Hohenstein, S. I. L. Kokkila, R. M. Parrish, and T. J. Martinez, *The Journal of Physical Chemistry B* **117**, 12972 (2013).
- [51] J. L. Whitten, *The Journal of Chemical Physics* **58**, 4496 (1973).
- [52] E. G. Hohenstein and C. D. Sherrill, *The Journal of Chemical Physics* **132**, 184111 (2010).
- [53] N. H. F. Beebe and J. Linderberg, *International Journal of Quantum Chemistry* **12**, 683 (1977).
- [54] H. Koch, A. S. de Meras, and T. B. Pedersen, *The Journal of Chemical Physics* **118**, 9481 (2003).
- [55] F. Aquilante, L. De Vico, N. Ferré, G. Ghigo, P.-r. Malmqvist, P. Neogrady, T. B. Pedersen, M. Pitoňák, M. Reiher, B. O. Roos, L. Serrano-Andrés, M. Urban, V. Veryazov, and R. Lindh, *Journal of Computational Chemistry* **31**, 224 (2010).
- [56] T. Helgaker, P. Jorgensen, and J. Olsen, *Molecular Electronic Structure Theory* (Wiley, 2002).
- [57] B. Peng and K. Kowalski, *Journal of Chemical Theory and Computation* **13**, 4179 (2017).
- [58] D. W. Berry, A. M. Childs, R. Cleve, R. Kothari, and R. D. Somma, in *STOC '14 Proceedings of the 46th Annual ACM Symposium on Theory of Computing* (2014) pp. 283–292.
- [59] G. H. Low and I. L. Chuang, *Physical Review Letters* **118**, 010501 (2017).
- [60] D. A. Mazziotti, *Physical Review Letters* **108**, 263002 (2012).
- [61] N. Rubin, R. Babbush, and J. McClean, *New Journal of Physics* **20**, 053020 (2018).
- [62] W. A. Al-Saidi, S. Zhang, and H. Krakauer, *Journal of Chemical Physics* **124**, 224101 (2006).
- [63] D. Vanderbilt, *Physical Review B* **41**, 7892 (1990).
- [64] V. Giovannetti, S. Lloyd, and L. Maccone, *Physical Review Letters* **100**, 160501 (2008).
- [65] R. Babbush, D. Berry, and H. Neven, [arXiv:1806.02793](https://arxiv.org/abs/1806.02793), 1 (2018).
- [66] J. R. McClean, R. Babbush, P. J. Love, and A. Aspuru-Guzik, *The Journal of Physical Chemistry Letters* **5**, 4368 (2014).

Appendix A: Cost of computing table lookups assisted by clean ancillae

In the case where clean qubits are used for the QROM, the steps are as follows.

- Given the address space size d and the output size M , choose a power of 2 chunk size k . These numbers will determine the space and time costs.
- Allocate registers r_0, \dots, r_{k-1} each with M clean qubits initialized to the $|0\rangle$ state.
- Let h be the superposed integer value of the top $\log(d/k)$ qubits of the address register. Perform a table lookup with address h targeting the r_0, \dots, r_{k-1} registers. The data for register r_l at address h is equal to the data from the original table at address $h \cdot k + l$. In effect, this is reading many possible outputs at once.
- Let l be the superposed integer value of the bottom $\log k$ qubits in the address register. Using a series of Wk controlled swaps, permute the registers r_0, \dots, r_{k-1} such that r_l ends up where r_0 was. The other registers can be permuted in any order.
- r_0 is now storing the output.
- Note that every computational basis value of the address register results in a specific computational basis value for registers r_0, \dots, r_{k-1} at this point. We have performed the equivalent of table lookup targeting r_0, \dots, r_{k-1} . We can use the uncomputation strategy from [Appendix C](#) to uncompute this effective lookup. The first thing done by that strategy is to measure all output qubits in the X basis. We will not be using any of the qubits from registers r_1, \dots, r_{k-1} until that point so they can be measured now instead of later. This frees the clean ancillae for other uses. Keep the measurement results so they can be used by the uncomputation process.

The swapping subroutine of this algorithm has a Toffoli count of $M(k-1)$. The table lookup subroutine has a Toffoli count of d/k . We perform each exactly once, therefore the total Toffoli count is $d/k + Mk$. The space cost of the procedure is M clean qubits to store the output, $(k-1)M$ clean ancillae for workspace, and $\log(d/k)$ clean ancillae hidden in the implementation of the table lookup subroutine.

The value of k that minimizes the Toffoli count is $\sqrt{d/M}$. In practice the number of available clean qubits often bounds k to be a much smaller value.

Appendix B: Cost of computing table lookups assisted by dirty ancillae

In [\[48\]](#) it is explained how to perform an efficient table lookup (a QROAM read) assisted by dirty ancillae. Here we summarize an equivalent technique, which proceeds as follows.

- Given the address space size d and the output size M , choose a power of 2 chunk size k . These numbers will determine the space and time costs.
- Allocate a register r_0 with M clean qubits in the $|+\rangle$ state. This register will ultimately store the output.
- Borrow registers r_1, \dots, r_{k-1} each of size M containing dirty ancillae.
- Let l be the superposed integer value of the bottom $\log k$ qubits in the address register. Using a series of Mk controlled swaps, permute the registers r_0, \dots, r_{k-1} such that r_0 ends up where r_l was. The other registers can be permuted in any order. Call this swapping procedure S .
- Let h be the superposed integer value of the top $\log(d/k)$ qubits of the address register. Perform a table lookup with address h targeting the r_0, \dots, r_{k-1} registers. The data for register r_l at address h is equal to the data from the original table at address $h \cdot k + l$. In effect, this is reading many possible outputs at once. Call this lookup process T .
- Perform the inverse of the swapping procedure S .
- Because r_0 was in the $|+\rangle$ state, it was not affected by T but all other registers were. Apply Hadamard operations to r_0 so that it will be affected by the next T , which will also uncompute the dirt XOR'ed into the other registers.
- Perform S then T then S^{-1} again.
- r_0 is now storing the output. The other registers are restored. Return the borrowed r_1, \dots, r_{k-1} registers.

The swapping subroutine S has a Toffoli count of $M(k-1)$. The table lookup subroutine T has a Toffoli count of d/k . We compute/uncompute S four times and perform T twice. Therefore the total Toffoli count is $2d/k - 2M + 4Mk$. The space cost of the procedure is W clean qubits to store the output, $(k-1)M$ dirty ancillae for workspace, and $\log(d/k)$ clean ancillae hidden in the implementation of T .

The value of k that minimizes the Toffoli count is $\sqrt{2d/M}$. In practice the number of available dirty qubits often bounds k to be a much smaller value. The value of k must be greater than 2 in order to have a Toffoli count lower than a standard lookup.

Appendix C: Efficient uncomputation of table lookups

Whenever a quantum circuit uncomputes a qubit q by performing a series of unitary operations that result in the qubit being in the $|0\rangle$ state, the circuit can be optimized by application of the deferred measurement principle. For example, suppose the last operation involving q is a CNOT targeting q . Then the circuit can be optimized by measuring q in the X basis before the CNOT, then replacing CNOT with a Z gate conditioned on the measurement result. This is an optimization because, in the surface code, Z gates require no spacetime volume.

This general pattern of “take an X -axis interaction that clears a qubit and use an X basis measurement and a classically-conditioned phase fixup operation instead” applies to many constructions, including table lookups. Let’s consider the nature of the phase fixup task we must perform when we eagerly measure the output qubits of a table lookup in the X basis.

We can think of each entry in the table as corresponding to a multi-control multi-target CNOT operation. There is one control (or anti-control) for each address qubit, and one target (or skip) for each output qubit. Because we will be measuring the output qubits, it is helpful to flip our perspective and think of the output qubits as the controls and the address qubits as the targets. For example, suppose the entry at address 2 of the table is the bit string 10011000. This means that the table lookup must toggle the qubits at offset 0, 3, and 4 of the target register conditioned on the address register storing 2. Or, equivalently, this means that the table lookup must negate the amplitude of the $|2\rangle$ state of the address register, conditioned on the $X_0 \cdot X_3 \cdot X_4$ observable of the qubits in the target register. Because we measured the output qubits in the X basis, we know the value of the $X_0 \cdot X_3 \cdot X_4$ observable and thus know whether or not we need to negate the amplitude of the $|2\rangle$ state of the address register. In fact, using the observables we measured, we can figure out for every state $|j\rangle$ of the address register whether or not $|j\rangle$ needs to be negated. Performing the necessary negations uncomputes the table lookup.

Let S be the set of all address register states that need to have their amplitude negated. This will be some arbitrary subset of the states from $|0\rangle$ to $|d-1\rangle$. We now transform the task of negating all the states in S into the task of performing a table lookup of size $d/2$ with output size 2. Let q be the least significant qubit of the address register, and u be a clean ancilla qubit in the $|1\rangle$ state. Apply a CNOT from q onto u , then apply a Hadamard transform to each. Now define a “fixup table” F with entries F_j each specifying two output bits defined by S :

$$F_j = \begin{cases} 00 & (2j \notin S) \wedge (2j+1 \notin S) \\ 01 & (2j \in S) \wedge (2j+1 \notin S) \\ 10 & (2j \notin S) \wedge (2j+1 \in S) \\ 11 & (2j \in S) \wedge (2j+1 \in S) \end{cases} \quad (\text{C1})$$

After preparing q and u , perform a table lookup from F onto q and u . The address of the lookup is all of the qubits of the address register, except for the least significant qubit. Because of how we defined F and how we prepared q and u , this negates the phase of all states from S . This uncomputes the table lookup, and we finish the uncomputation by uncomputing the preparation of q and u . See [Figure C](#) for a quantum circuit showing an overview of the process.

This technique implements the uncomputation of a table lookup with address size d and output size M in terms of computing a table lookup with address size $d/2$ and output size 2. Reducing the address and output size increase the effectiveness of the techniques explained in [Appendix A](#) and [Appendix B](#), since a larger value of k can be used.

By combining this technique and [Appendix A](#), if k additional clean ancillae are available, the Toffoli cost of uncomputing a table lookup with address size d and output size M can be reduced to $d/k + k$. This equation is minimized at $k = \sqrt{d}$, where the Toffoli count is $2\sqrt{d}$. k should be a power of two.

Combining this technique with [Appendix B](#) instead, if k additional dirty ancillae are available, the Toffoli cost of uncomputing a table lookup with address size d and output size M can be reduced to $2d/k + 4k$. This equation is minimized at $k = \sqrt{d/2}$, where the Toffoli count is $\sqrt{32d}$. k should be a power of two.

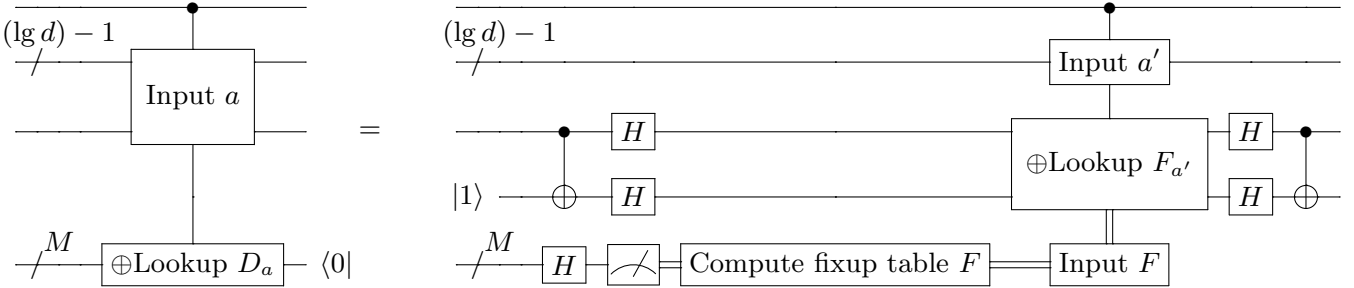


FIG. 2. Uncomputing a table lookup using eager measurement and phase fixups. Reduces the effective address size from d to $d/2$ and the effective output size from M to 2.

Appendix D: Rank reducing the FeMoco Coulomb operator

Here we discuss the procedure for choosing the value of L for our FeMoco calculations. Our approach is to choose L by observing the effect of truncation on two different efficient classical correlated approximate methods for molecular electronic structure: Configuration Interaction at the singles and doubles level (CISD) and Møller-Plesset perturbation theory to second order (MP2). For a review of both methods, see [\[56\]](#), or any other quantum chemistry textbook.

We perform CISD/MP2 on the exact Hamiltonian and then perform CISD/MP2 on the truncated Hamiltonian for various truncations and track the discrepancy. We plot how the energies converge for the Reiher *et al.* [\[33\]](#) and Li *et al.* [\[49\]](#), in [Figure 3](#) and [Figure 4](#), respectively. Specifically, we plot the correlation energy (the difference between the mean-field energy and the exact energy) for the sole reason that the mean-field energy converges much faster than the correlation energy and so it is easier to see the trend this way. In general, CISD and MP2 are very different methods and we would expect truncation to affect them differently. However, both methods appear extremely well converged, for both Reiher and Li integrals, by $L = 200$. This gives us confidence that the exact ground state energy of the truncated Hamiltonian would also be consistent with the exact ground state energy of the untruncated Hamiltonian by this point. Accordingly, we choose 200 as the rank of our Coulomb operator. Note that the Reiher and Li integrals have very different properties, and so we assume it is a coincidence that both converge around the same value of L .

Finally, we note that even this truncation procedure might be overly conservative. In practice, it is widely observed that there is significant cancellation of errors that occurs across energy landscapes when using molecular orbitals. Very often, the difference in ground state energies between two distinct nuclear geometries is more accurate than the single-point energy at either of those geometries. Thus, because differences in energies are all that matter in this context, we might find substantial cancellation of truncation errors across different geometries.

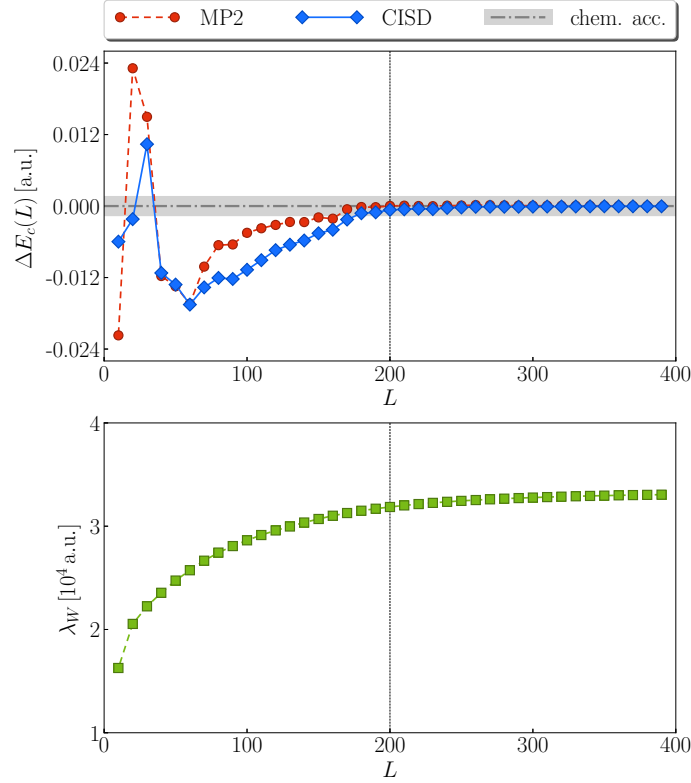


FIG. 3. Top: difference ΔE_c between truncated and untruncated correlation energy, for the FeMoco cluster, using the 108 spin-orbital active space from Reiher *et al.* [33], and MP2 and CISD methods (red, blue). The grey shaded region represents chemical accuracy; thus, we expect $L = 200$ is sufficient for our purposes. Bottom: λ_W as a function of L . For this system $\lambda_T = 1,490$ a.u., $\lambda_V = 8,373$ a.u. and the maximum value of λ_W is 34,552 a.u.; thus, we take $\lambda = 36,042$ a.u.

Appendix E: Exploiting sparsity in the Coulomb operator

In this appendix we discuss a strategy for further reducing constant factors when qubitizing either the factorized, or unfactorized quantum chemistry Hamiltonians. This strategy will likely reduce the T complexity in practical situations, but only by constant factors. As in the main paper we focus on two forms of the Coulomb operator:

$$V = \sum_{\alpha, \beta \in \{\uparrow, \downarrow\}} \sum_{p, q, r, s=1}^{N/2} V_{pqrs} a_{p, \alpha}^\dagger a_{q, \alpha} a_{r, \beta}^\dagger a_{s, \beta}, \quad W = \sum_{\ell=1}^{N^2/4} \omega_\ell \left(\sum_{\sigma \in \{\uparrow, \downarrow\}} \sum_{p, q=1}^{N/2} g_{pq}^{(\ell)} a_{p, \sigma}^\dagger a_{q, \sigma} \right)^2, \quad (\text{E1})$$

where we note that for the purposes of this appendix the sum over ℓ in W is not truncated and goes to $N^2/4$. Here we will also discuss a different type of truncation for both operators. We define these truncations as

$$\tilde{V}^{(c)} = \sum_{\alpha, \beta \in \{\uparrow, \downarrow\}} \sum_{p, q, r, s=1}^{N/2} \tilde{V}_{pqrs}^{(c)} a_{p, \alpha}^\dagger a_{q, \alpha} a_{r, \beta}^\dagger a_{s, \beta}, \quad \tilde{V}_{pqrs}^{(c)} = \begin{cases} V_{pqrs}, & |V_{pqrs}| \geq c, \\ 0, & |V_{pqrs}| < c, \end{cases} \quad (\text{E2})$$

$$\tilde{W}^{(c)} = \sum_{\ell=1}^{N^2/4} \omega_\ell \left(\sum_{\sigma \in \{\uparrow, \downarrow\}} \sum_{p, q=1}^{N/2} \tilde{g}_{pq}^{(\ell, c)} a_{p, \sigma}^\dagger a_{q, \sigma} \right)^2, \quad \tilde{g}_{pq}^{(\ell, c)} = \begin{cases} g_{pq}^{(\ell)}, & \omega_\ell |g_{pq}^{(\ell)}|^2 \geq c, \\ 0, & \omega_\ell |g_{pq}^{(\ell)}|^2 < c. \end{cases} \quad (\text{E3})$$

The purpose of these truncations is to induce sparsity in the operators by removing near-zero elements. The idea of reducing quantum simulation costs by exploiting sparsity in the Coulomb operator was first explored in [66], but in the context of Trotter based methods. The idea of the approach here is to choose the value of c to be as large as possible while still leaving classical correlated approximations such as CISD within chemical accuracy (essentially the same procedure we used for choosing L shown in Figure 3 and Figure 4).

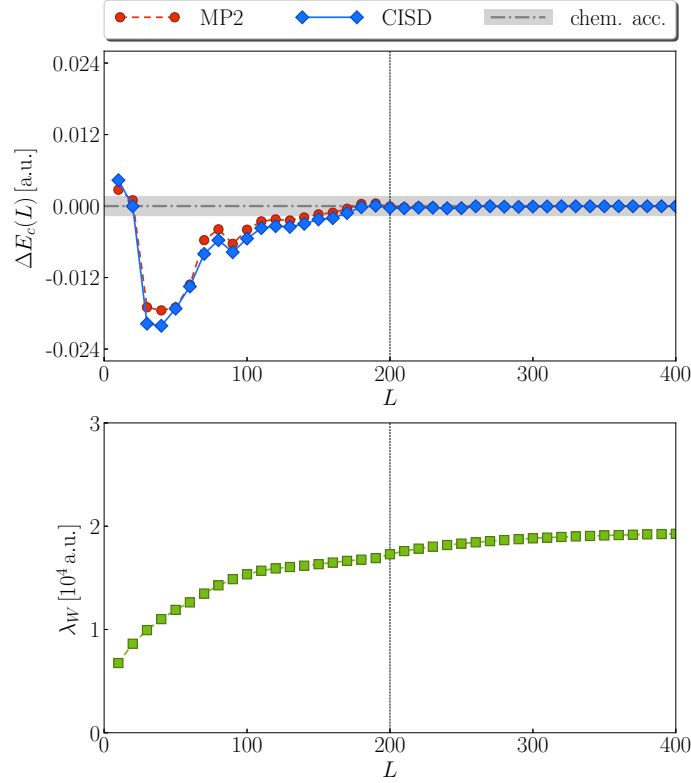


FIG. 4. Top: difference ΔE_c between truncated and untruncated correlation energy, for the FeMoco cluster, using the 152 spin-orbital active space from Li *et al.* [49], and MP2 and CISD methods (red, blue). The grey shaded region represents chemical accuracy; thus, we expect $L = 200$ is sufficient for our purposes. Bottom: λ_W as a function of L . For this system $\lambda_T = 3,446$ a.u., $\lambda_V = 4,168$ a.u. and the maximum value of λ_W is 20,746 a.u.; thus, we take $\lambda = 24,192$ a.u.

We will define $L_V^{(c)}$ as the number of nonzero values of $\tilde{V}_{pqrs}^{(c)}$ and $L_W^{(c)}$ as the number of nonzero values of $\tilde{g}_{pq}^{(\ell,c)}$. In general, we expect that $L_V^{(c)} = \mathcal{O}(N^4)$ and $L_W^{(c)} = \mathcal{O}(N^3)$; which is to say that these truncations should not asymptotically change the sparsity of the operators. However, in practice we do expect to find that $L_V^{(c)} < N^4/16$ and $L_W^{(c)} < N^2L/4$; which is to say that we do expect there to be additional sparsity in these operators. While the matter of exactly how much sparsity exists is highly system dependent, we might sometimes desire an algorithm that exploits this sparsity, even if it is highly unstructured.

It is possible to perform a state preparation that has cost dependent on the number of nonzero elements, at the cost of a slightly larger number of ancillae. Consider the state preparation of [13], which has the following steps.

1. Create an equal superposition over the system registers

$$\frac{1}{\sqrt{d}} \sum_{j=1}^d |j\rangle. \quad (\text{E4})$$

2. Use QROM indexed on the system registers to output alt values and keep values

$$\frac{1}{\sqrt{d}} \sum_{j=1}^d |j\rangle |\text{alt}_j\rangle |\text{keep}_j\rangle. \quad (\text{E5})$$

3. Use another ancilla in an equal superposition over 2^μ values where μ is the number of digits for keep. Perform an inequality test between this register and the keep register, and swap the contents of the first two registers (the index and alternative index registers) based on the result of this inequality test.

The total number of ancillae used by this state preparation is $2\lceil \log d \rceil + 2\mu + 1$. It is also possible to save a qubit by inverting the inequality test to erase the qubit storing the result of the inequality test.

In order to perform the preparation in the sparse case, instead of iterating over the index register, we can output the index register in the same way as the alternate index register. That is, we have a register which iterates over the number of nonzero amplitudes in the state we aim to prepare. Say that number is s ; then our steps are as follows.

1. Create an equal superposition over the register indexing the nonzero entries.

$$\frac{1}{\sqrt{s}} \sum_{j=1}^s |j\rangle. \quad (\text{E6})$$

2. Use QROM indexed on this first register to output ind, alt, and keep values

$$\frac{1}{\sqrt{s}} \sum_{j=1}^s |j\rangle |\text{ind}_j\rangle |\text{alt}_j\rangle |\text{keep}_j\rangle. \quad (\text{E7})$$

3. Use another ancilla in an equal superposition over 2^μ values, and perform an inequality test between this register and the keep register. Based on the result of this inequality test, swap the contents of the ind and alt registers.

The desired state will then be produced in the second register where we output ind. The value ind_j is simply the index for the j th nonzero amplitude. The correctness of this state preparation routine follows immediately from the correctness of the routine in [13], because after the QROM lookup the state in the registers excluding the first is equivalent to that in [13]. The Toffoli complexity of this modified state preparation procedure for sparse states is equal to the number of nonzero entries s plus the number of qubits for the keep register μ . The number of ancillae is increased by $\lceil \log s \rceil$.